ANALYSIS OF SUPERNOVA Ia PROGENITOR SYSTEMS: White Dwarf-Main Sequence Binaries, Cataclysmic Variables, and the Symbiotic Stars LIN 358 and SMC N73

Jasmin Washington
Supervisor: Professor Steven Majewski

Department of Astronomy
University of Virginia
May 7, 2020

This thesis is submitted in partial completion of the requirements of the
BS Astronomy-Physics Major

Draft version May 8, 2020
Typeset using LaTeX **twocolumn** style in AASTeX63

ABSTRACT

Type Ia supernovae (SNe Ia) occur when a white dwarf (WD) in a binary becomes unstable and explodes, but the exact path to this event is unknown. One possible channel, the single degenerate scenario, is that the WD accretes mass from its companion until the WD reaches the Chandrasekhar limit ($1.4M_{\odot}$) and explodes. Another channel, the double degenerate scenario, sees a merger between two WDs that results in an explosion. A way to study the progenitor scenarios is by examining Cataclysmic Variables (CVs), a type of white dwarf-main sequence (WD-MS) binary. To tackle the study and discovery of more WD-MS binaries, the spectral energy distributions (SEDs) of sources in the APOGEE-GALEX-*Gaia* SN Ia Progenitor Catalog are visually classified and sorted to identify these systems. The methodology used to create the catalog was found to be effective for finding WD-MS binaries. In the second part of this thesis, two sources within this catalog, the symbiotic stars LIN 358 and SMC N73, are characterized using WHACCKEY PAR (WHite dwarf And Companion Characterization of KEY PARameters), a Python SED model fitting pipeline and the custom Monte Carlo sampler *The Joker*. The period of LIN 358 was well constrained and was found to have a highly elliptical orbit. Follow up observations of SMC N73 would allow better characterization and could identify potential X-ray emission.

Keywords: Stars: binaries: symbiotic; Astrophysics - Solar and Stellar Astrophysics

1. INTRODUCTION

Type Ia supernovae (SNe Ia) occur when a white dwarf (WD) in a binary becomes unstable and explodes, either due to reaching the Chandrasekhar limit through accretion or a merger with the other white dwarf within a WD-WD binary system. SNe Ia are fundamental to our understanding of astronomy. For example, they serve as standard candles for measuring cosmological distances and the expansion rate of the universe with their characteristic light curve, and also as calibrators for cutting edge gravitational wave detectors. But the progenitors for these explosions remain one of the biggest mysteries in astronomy.

One theory for how SNe Ia occur is the single degenerate scenario, where a white dwarf in a binary accretes mass from its nondegenerate (main sequence or MS) companion until it exceeds the Chandrasekhar limit (1.4 $M_{\odot}$) and explodes. One way to study this single progenitor scenario is by examining Cataclysmic Variables (CVs), short period (down to the scale of hours) interacting binaries that contain a primary white dwarf accreting mass from a secondary companion star that fills the Roche-lobe. The double degenerate scenario begins when the nondegenerate companion to the WD expands and becomes a giant. Eventually the expanding gas envelope engulfs both stars, and the orbital energy of the binary unbinds the envelope from its host, leaving behind a WD core. The separation of the two WDs shrinks and eventually they inspiral and merge, causing a SNe Ia.

Because there are many white dwarfs both within our galaxy and its satellites, with many undergoing accretion at nonrelativistic speeds, there should be several CVs within our galaxy. Studying CVs as progenitors of SNe Ia provides useful insight for both the single and double degenerate scenarios, since the double progenitor scenario of SNe Ia begins with the WD and nondegenerate companion of the single degenerate scenario.

Going a step further back, by studying the progenitors of CVs it is possible to gain insight into the different evolutionary pathways for the WD in the binary. Such a study requires a catalog of WD-MS binaries, which become CVs once the companion fills the Roche-lobe. We intend to undertake a study of a specific subsample of these WD-MS systems that exhibit a clear UV excess from an extremely hot WD accreting mass from its main sequence companion. Our study takes advantage of a unique catalog of WD-MS candidates, the APOGEE-GALEX-*Gaia* SN Ia Progenitor Catalog, recently created for the purpose of finding CV candidates. In the first part of this thesis, Section 2, the assembly of this catalog is discussed and we undertake a preliminary assessment of its contents via visual inspection of the spectral energy distributions (SEDs) of members to identify a clear UV-excess and potential CV candidates.

BINARY	α	δ
LIN 358	$00^h59^m12.251313^s$	$-75^h05^m17.616419^s$
SMC N73	$01^h04^m39.306394^s$	$-75^h48^m24.765843^s$
Draco C-1	$17^h19^m57.657086^s$	$+57^h50^m05.482634^s$

Table 1. Sexagesimal coordinates of the three symbiotic stars of interest. Retrieved from Merc et al. (2019).

Identified among these candidates were three particularly interesting targets: LIN 358, SMC N73, and Draco C-1 (coordinates in Table 1). They are confirmed symbiotic stars (SySts) in satellite dwarf galaxies. Symbiotic stars are interacting binary systems composed of a hot compact companion accreting at a high rate from a red giant or supergiant, which frequently fills its Roche lobe. When the compact companion is a WD, the companion is either a red giant or an asymptotic giant branch (AGB) star (Akras et al. 2019). The supersoft X-ray emission observed from LIN 358 and Draco C-1 is from the steady nuclear burning of hydrogen accreted onto the surface of the WD (Skopal 2015). Analyzing Draco C-1 will be presented in Lewis et al. (in prep). The second part of this thesis is the analysis of the other two systems, which we describe in Section 4 using the methods outlined in Section 3.

2. VISUAL CLASSIFICATION

This section will discuss the APOGEE-GALEX-*Gaia* SN Ia Progenitor catalog, specifically how it was assembled and the visual classification that was performed on the spectral energy distributions (SEDs) of the potential CVs.

2.1. *APOGEE-GALEX-Gaia SN Ia Progenitor Catalog*

A catalog of 1470 CV candidates was classified by visual inspection of the SEDs. These candidates were selected for the APOGEE-GALEX-GAIA SN Ia Progenitor Catalog because they show a significant brightness in the UV (see Figure 1).

The APO Galactic Evolution Experiment (APOGEE) survey (Majewski et al. 2017) is a large infrared spectroscopic census of the chemistry and radial velocities of stars, data that are intended to help determine how the Galaxy evolved. The effective temperatures provided by APOGEE helped with identification of white dwarf main sequence (WD-MS) candidates. Meanwhile, the Galaxy Evolution Explorer (GALEX) is a space telescope launched on April 28th, 2003 with the goal of understanding the evolution primarily of *other* galax-

ies. The value of GALEX relevant to this project is the study of stellar evolution in the UV range (Morrissey et al. 2007). The NUV (effective $\lambda \sim 2304.7$ Å) and FUV (effective $\lambda \sim 1549.0$ Å) filters of GALEX make it sensitive to very hot stars of the type we seek as critical elements of CV candidates. The ultraviolet magnitudes for the (FUV-NUV) color were provided by the GALEX catalog (Bianchi et al. 2017, with corrections from Wall et al. 2019 for the brightest targets).

Gaia Data Release 2 (DR2) (Gaia Collaboration et al. 2018) contains astrometry (parallaxes and proper motions) for 1,692,919,135 sources. It also contains median radial velocities for 7.2 million stars. Parallax measurements from *Gaia* were used to find the distances to the sources. The photometry in *Gaia* DR2 also comprises some of the observations in the source SEDs.

The APOGEE-GALEX-*Gaia* catalog was assembled by Dr. Borja Anguiano by combining the *H*-band APOGEE DR16 data set with the GALEX UV photometry provided by GALEX and the astrometric data from *Gaia*. Using the combination of the spectroscopically-derived stellar temperatures from APOGEE and the ultraviolet photometry from GALEX, it was possible to identify F, G, and early K and M main sequence stars with a bluer FUV-NUV color than is observed for a single star. This brightness in the UV may be caused by the presence of a nearby, hot companion such as a white dwarf. This distinction is shown visually in Figure 1. The red triangles represent the FUV-NUV colors for a given temperature, metallicity and surface gravity for single stars in the UVBLUE synthetic spectrum library (Rodríguez-Merino et al. 2005), and the significantly blueward points enclosed by the blue circle are the targets in the APOGEE-GALEX-*Gaia* catalog. The red line is an arbitrary boundary separating the single stars and WD-MS binary candidates. The sample was then further refined by selecting for stars in the multi-epoch APOGEE spectra having radial velocity (RV) scatter larger than reported errors, a quality which confirms they are binaries. Pulsating RR Lyrae and Cepheid variable stars are warm, have (FUV-NUV) colors around 3 to 5 (Kinman & Brown 2014) like the WD-MS binary candidates, and also have RV variability. Because of this, variable stars are potential contaminants in the catalog. They were removed by only keeping sources with $T_{eff} < 5700$ K in the catalog, since the average temperature of these variable stars is around 6000 K (Kolenberg et al. 2010).

While Figure 1 seems a promising way to search for interesting WD-MS sources, we want to test the methodology with a visual inspection of the source spectral energy distributions (SEDs).

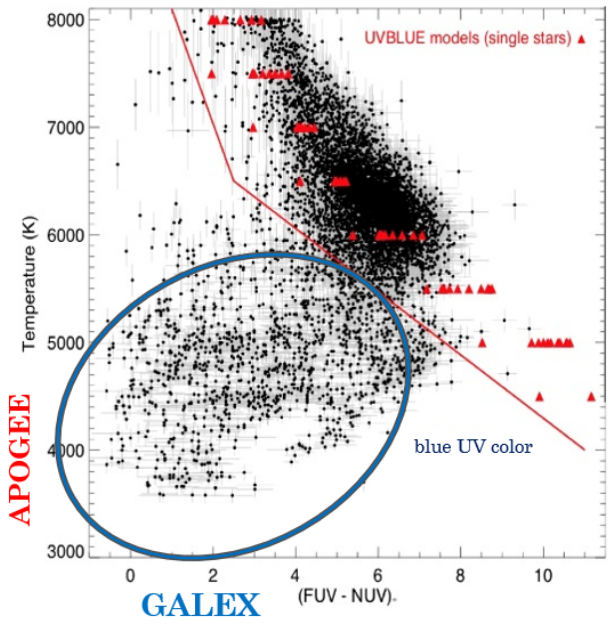

Figure 1. Graph depicting the effective temperature from APOGEE and (FUV-NUV) color from GALEX for sources. The group above the red line is composed of single, non-variable stars. The group within the blue circle are high probability WD-MS candidates as the significant brightness in the UV could be from a hot companion.

2.2. *SED Creation and Classification*

Having identified a sample of main sequence sources likely to be harboring white dwarf companions (Fig. 1), we want to further assess their validity through a more careful examination of their full SED.

The SEDs were created on the Virtual Observatory SED Analyzer (VOSA) website (Bayo et al. 2008). They were constructed from existing photometry on the targets by accessing numerous catalogs and retrieving the flux in $erg/cm^2/s/A$ at all available wavelengths for a target, ranging from the UV to the infrared. Then, to understand the expected UV contribution to the SED coming from the main sequence star, BT-Settl-CIFIST models (Baraffe et al. 2015) for the MS stars in the binaries were applied and tested using a χ^2 goodness-of-fit test. This SED-fitting was done automatically by VO, and the BT-Settl-CIFIST model with the smallest χ^2 for each target was visually classified based on how well the observed FUV and NUV flux fit that of the model. The GALEX *FUV* and *NUV* fluxes were not removed from the points used in the fit, so this likely had an effect on the resulting model fits and SEDs that were classified. The reason these points were not removed was that for some targets VO gave an error stating there was insufficient data for the fit without the two points.

After a first pass visual inspection of the results of the automated SED-fitting exercise, it was clear that most of the SEDs for these systems fell into five morphological classes, as shown by the examples in Figure 2. Type 1 SEDs show a clear excess of UV flux from the white dwarf. Variable 1 (V1) SEDs also appear to possess excess UV flux, but erratic behavior in the flux at longer wavelength makes it difficult to get a good fit of the BT-SETL models to the data. This "bumpiness" in the SED may be due to intrinsic object variability or mean observed fluxes with large errors. If the object was flaring at the time of observation there would be more flux at these points, causing the bumpiness. Type 2 SEDs have either only excess flux in the FUV filter or are perfectly modeled by a MS star. These are sources that could have a WD in a binary, but it is faint and the MS star dominates the NUV. Variable 2 (V2) are the Type 2 version of V1, barely or not at all showing excess UV flux but also exhibiting an MS model offset due to varying longer wavelength fluxes. A fifth category, "Unclassified," represent those objects that cannot be easily sorted into the other four categories.

The final results of the visual SED classification are that there were 476 Type 1, 518 Type 2, 164 V1, 122 V2, and 190 Unclassified SEDs. The Type 1 and V1 SEDs show the most promise for being CV systems and warrant further investigation and observation, although a few have already been identified as galaxies (Seyferts, active galactic nuclei) in follow up cross matching of the Type 1 source coordinates with the SIMBAD astronomical database. The Unclassified SEDs could also be worth further investigation to determine what these objects are. By performing this visual classification of the SEDs, those in the Type 2 and V2 categories can be removed from the catalog as the least interesting, which improves the efficiency of any follow-up efforts.

Of the 1470 CV candidates selected from Figure 1, 43% were Type 1 (32%) or V1 (11%), showing that the methodology used to create the APOGEE-GALEX-*Gaia* SN Ia Progenitor catalog is in fact effective for finding promising WD-MS candidates and possible CV systems. Through this process of SED fitting and categorization, the strongest candidates for WD-MS binaries and possible CV systems were identified along with "unclassified" targets where further investigation both in databases and observations could yield interesting results.

A second result of the SED categorization effort in this section was the confirmation of the sources LIN 358 and SMC N73 as systems containing extremely hot stellar components. A deeper analysis of the SEDs for these two systems is the goal of the second part of this thesis.

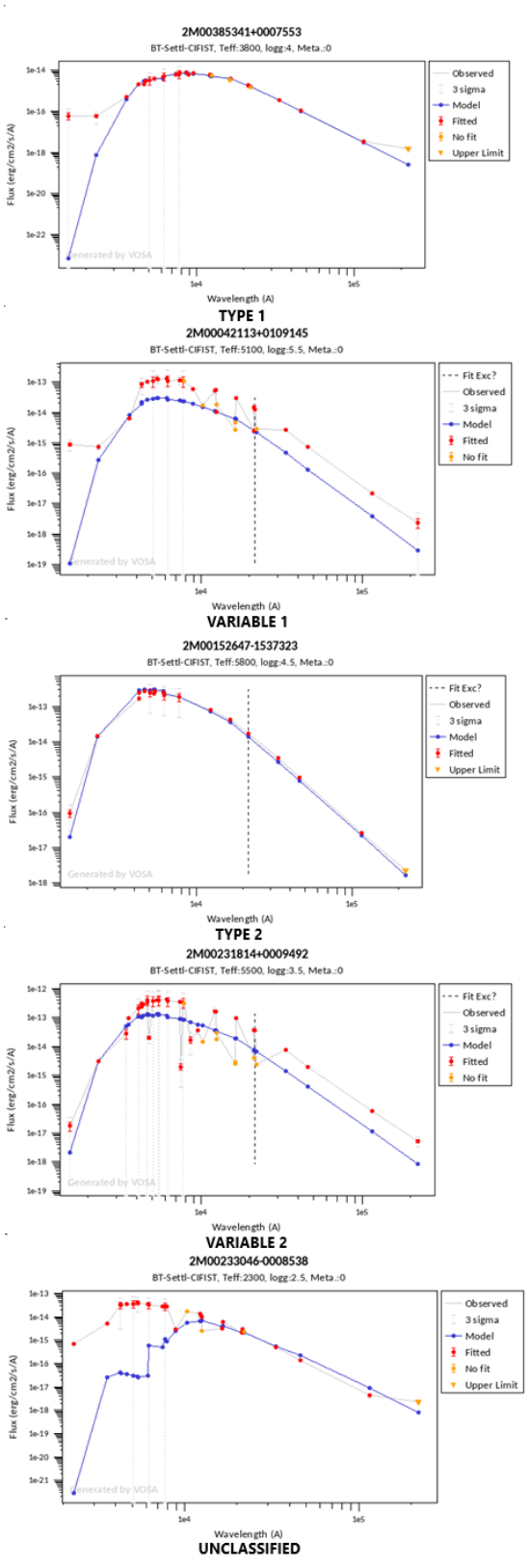

Figure 2. Example SEDs that were created in Virtual Observatory from each of the five morphological classes.

3. IMPROVED SED MODEL FITTING

After visual inspection of the automatically-generated SED fitting described in Section 2, it became clear that a more precise flux analysis of these systems was necessary if one is to derive astrophysical information from the stellar SEDs. The BT-Settl-CIFIST model fits from VOSA are a good approximation for the MS-dominated portion of the SED that enables the identification of excess UV flux, but APOGEE provides accurate values for the temperature, $\log g$, and metallicity of the companion to the WD from high resolution spectroscopy. Also, in both LIN 358 and SMC N73 the cooler companions are giants, meaning the BT-Settl-CIFIST model library, which models main sequence stars, is not appropriate to use. By using values for the giant companion from APOGEE, there are less free parameters in the fitting process, so characterization of the WD with the Python pipeline WHACCKEY PAR (WHite dwarf and Companion Characterization of KEY PARameters) will produce a more accurate estimate for the WD temperature and the radius of both the giant and white dwarf.

WHACCKEY PAR, developed and discussed here in Section 3.1, is designed to fit a WD and a MS star or giant companion. The Kurucz model library (Kurucz 1993 with corrections by Castelli et al. 1997) contains a wide enough range of values for T_{eff}, $\log(g)$, and metallicity that both a main sequence star and giant can be fitted using the library. To fit the fluxes of the white dwarf, a library of blackbody (BB) (Bayo et al. 2008) models was used.

Another pipeline used to characterize the binary is the Monte Carlo sampler *The Joker*, which is able to provide constraints on Keplerian parameters from sparse or noisy radial velocity measurements for a two-body system with as few as three epochs (Price-Whelan et al. 2017). This sampler is discussed further in Section 3.3.

3.1. *WHACCKEY PAR*

The giant and white dwarf in the binary were characterized individually using synthetic photometry libraries from Virtual Observatory. These synthetic photometry libraries were created by convolving the filter functions for the 5839 astronomical filters available in the VO Filter Profile Service with the theoretical spectra. This allows better characterization/model fitting of SEDs for real astronomical sources than fitting with the theoretical spectra because the fluxes in the models more closely resemble actual observations than the idealized fluxes in spectra. Described another way, the synthetic photometry is designed to make it seem as if the theoretical model libraries were observed and not calculated with ideal conditions.

For the giant, the Kurucz model with the closest values for $\log(g)$, temperature, and metallicity to the APOGEE data was used. The Kurucz synthetic photometry library contains models spanning metallicities ranging from -2.5 to +0.5, $\log(g)$ from 0.0 to 5.0, and effective temperatures of 3500 to 6500 K. For the BB/WD SED fitting, the temperature range used in WHACCKEY PAR is from 100,000 K to 200,000 K with increments of 1000. Available models in the BB synthetic photometry library cover temperatures from 10 to 200,000 K.

WHACCKEY PAR tests different models to see how well they fit the flux from the WD, but to do this we have a free parameter, γ, the dimensionless factor needed to match the model to the data. There are two scaling factors, one for the giant, α, and one for the WD, β. A χ^2 goodness-of-fit test was used to determine the best fitting model, signified by the minimum of:

$$\chi^2 = \sum_{i=1}^{N} \left[\frac{F_{obs}(\lambda_i) - \gamma * F_{mod}(\lambda_i)}{\Delta F_{obs}(\lambda_i)} \right]^2 \quad (1)$$

where $F_{obs}(\lambda_i)$ is the observed flux of the target at a given wavelength/filter, $\Delta F_{obs}(\lambda_i)$ is the error of the observed flux that weights the difference, and $F_{mod}(\lambda_i)$ is the flux of the model at the same wavelength. γ is a placeholder for the appropriate scaling factor. Since the wavelengths of the points in the model did not line up exactly with the wavelengths of the observations, $F_{mod}(\lambda_i)$ had to be interpolated for the χ^2. This was done using `scipy.interpolate.interp1d` to make the model into a 'function,' essentially flux as a function of wavelength, that could then be evaluated at the wavelengths of the observations. The scaling factors, α and β, were determined by dividing the observed flux by the model's flux at the same wavelength (see Eq. 2). The weighted differences were summed along a certain wavelength range for each object (see §3.1.1 and 3.1.2). These filters/wavelengths were chosen in such a way that the flux measured is dominated by one of the stars with minimal contribution by the other star.

The smallest χ^2 value from this comparison for a given model was then compared to the current smallest χ^2 and saved for comparison with future models if it was smaller. The model with the minimum χ^2 then had its wavelengths, corresponding fluxes, scaling factor and filename returned by the function. The scaling factor expressed mathematically is

$$\gamma = \frac{F_{obs}(\lambda)}{F_{mod}(\lambda)} = \left(\frac{R}{D}\right)^2 \quad (2)$$

Using this equation it is possible to calculate the radius, R, of the star if the distance to the system, D, is known.

3.1.1. *Giant Star Fit Specifications*

For the red giant in each system, χ^2 was calculated with α at the 2MASS K_s, WISE $W1$, WISE $W2$, and WISE $W3$ filter wavelengths to see which gave the smallest value for the model with parameters closest to the APOGEE data values. The wavelength range for the χ^2 test began at the effective wavelength for the 2MASS J filter and ended at the longest/reddest wavelength the binary was observed. The starting wavelength, 2MASS J (12350 Å), was chosen both because the white dwarf is minimally contributing to the flux at this point in the SED and also because the plots of observed flux for both binaries are smoothest within this range.

Once the radius R has been calculated from Equation 2, the mass M of the giant can then be calculated using its $\log(g)$ value in

$$\log(g) = \log\left(\frac{GM}{R^2}\right) \tag{3}$$

where G is Newton's gravitational constant in cgs units.

The $\log(g)$, temperature, and metallicity of the model used for the giant were used to retrieve the data for the corresponding Kurucz theoretical spectrum. This theoretical spectrum is the blue line plotted in the figures of Section 4 and its fluxes were used for calculating the total flux from the binary (a process explained in more depth in §3.2). The reason the fluxes from the spectrum were used for plotting and calculations instead of the fluxes from the synthetic photometry is that the spectrum is smoother, or has less outlier points that create sharp spikes in the plot of the flux. The exact source of these "spikes" is unknown, but can be easily smoothed as is done with the blackbody synthetic photometry.

3.1.2. *Blackbody Fit Specifications*

The phenomenon mentioned at the end of the last section, outlier data points or "spikes," are also seen in what should be a smooth blackbody function. These outliers could affect the χ^2 fit with large differences between the model and observed flux, affecting the quality of the fit. For fitting a model to the giant the outliers were less of an issue since the parameters for the model ($\log(g)$, temperature, and metallicity) were already known and a majority of the outliers were outside of the χ^2 summation range, but for the WD the temperature is unknown so the outliers should be smoothed out to ensure a better fit. To do this, the wavelengths and their corresponding fluxes were sorted by ascending wavelength. Then, the difference between a given point y[z] and the next point y[z+1] was calculated. If the absolute value of this difference was greater than the threshold, $2.4*(y[z]/10)$, the flux for y[z+1] was changed to that of y[z]. This was done for the first 3000 wavelengths, as this smoothed the majority of the spikes and avoided smoothing large differences caused by gaps in the data at longer wavelengths.

For the blackbody, the scaling factor β was calculated at the effective wavelengths for the GALEX FUV and GALEX NUV filters to see which gave the smaller χ^2. The range of summation for Equation 1 was all wavelengths less than 3600 Å. This was done to give the χ^2 test a couple of points to sum over without going too far into the domain where the giant is also heavily contributing to the observed flux.

The temperature of the best fitting blackbody model's synthetic photometry was plugged into the `blackbody_lambda` function from `astropy.modeling.blackbody` and the flux was calculated for the wavelength range of the model (Astropy Collaboration et al. 2013). Similar to the use of the Kurucz theoretical spectrum for the giant instead of the synthetic photometry, this smooth blackbody model is the red line plotted in Section 4 and its flux was used to determine the summed flux of the two models in Section 3.2.

3.2. *Total Flux*

Once the best fitting models for the giant and blackbody/WD were determined individually, the sum of the two models could be calculated to determine the total flux of the binary. Similar to how the flux of the model and observations had to be at the same wavelength for the χ^2 test, the flux of the BB or giant model had to be interpolated at the wavelengths of the other. It was decided the flux would be interpolated for the blackbody model since it covered a smaller wavelength range than the Kurucz spectrum and also because blackbody flux is easily calculated by Planck's Law:

$$B(\lambda, T) = \frac{2hc^2}{\lambda^5}\frac{1}{e^{\frac{hc}{\lambda k_B T}} - 1} \tag{4}$$

The values h and c are Planck's constant and the speed of light respectively. The interpolation was done using the same method described in Section 3.1, using the `scipy.interpolate.interp1d` function to turn the blackbody model into a function that could be evaluated at wavelengths/points in the Kurucz spectrum that do not have data in the blackbody model. With the wavelengths now matched between the two models, the total flux F_{tot} could then be determined from

$$F_{tot} = F_{Giant} + F_{WD} = \alpha * F_{Kurucz} + \beta * F_{BB} \tag{5}$$

where α and β are the scaling factors for the giant and white dwarf respectively. The scaling factors are neces-

sary for fitting models to the observations, but conceptually they also scale the flux from the two stars in the binary to match the actual contributions of the WD and giant to the total observed flux

Now that the workings of WHACCKEY PAR have been outlined, it can be applied to characterize the two symbiotic binaries LIN 358 and SMC N73 in Section 4.

3.3. *Joker Analysis*

The Joker uses radial velocity observations from APOGEE to provide constraints on six Keplerian parameters for binary systems, but the four relevant to this thesis are: period P, eccentricity e, velocity semi-amplitude K, and systemic velocity v_0. To further explain these, P and e are the period and eccentricity of the system. The velocity semi-amplitude K is the amplitude of the variation in the giant's velocity. The systemic velocity is the velocity of the binary's center of mass as it orbits the center of its host galaxy. Table 1 in Price-Whelan et al. (2020) gives the other parameters provided by *The Joker* along with their prior probability distribution functions (pdfs). If the mass of the primary (giant) is available, it is then possible to determine the companion (WD) mass.

The current version of *The Joker*, described in Price-Whelan et al. (2017), generates a set of dense prior samples using prior probability distribution functions for the orbital parameters. The prior samples span a user-defined range and each have a fixed P, e, K, v_0, etc. Next, random blocks of these prior samples from a cache of 100,000,000 are evaluated by *The Joker* to see how well each sample within the subset fits the data. The worst fitting prior samples are rejected, and this process continues until a user-defined number (in this case 256) of prior samples remain. These best-fitting samples are the posterior samples (blue lines) shown in Figures 4 and 6. The values returned for P, e, K, v_0, etc. are the values of the most likely (best fitting) sample, and its errors are given by the standard deviation of the 256 (or user-defined remaining number of) posterior samples.

Using *The Joker*, it was only possible for the Price-Whelan et al. (2020) analysis, the Joker APOGEE Value-Added Catalog (VAC), to characterize populations of binaries statistically rather than individual systems with posterior sampling. The main reason for this is that APOGEE always intends to gather multi-epoch RV data to identify binary stars, but typically does not collect enough epochs to characterize them, except in a statistical way. APOGEE employs strict cadencing requirements precisely to make sure they have sensitivity to binary stars, but with the nominal three visits for most stars and a limited survey timescale, it is impossible to be sensitive to all parts of parameter space. A total of 232531 unique APOGEE sources were able to be characterized in the VAC using *The Joker*.

4. SYMBIOTIC STARS

LIN 358 and SMC N73 are two known symbiotic stars (SySts) in the Small Magellanic Cloud (SMC). They are both classified as stellar or S-type binaries based on their near-infrared (IR) data. S-type binaries have a near-IR color temperature of $\sim 3000 - 4000$ K, a result of a K, M, or G spectral-type giant. D and D'-type have a near-IR color temperature of only 700-1000 K, indicating a warm dusty envelope surrounding an evolved asymptotic giant branch (AGB) star. This means S-types, and by extension LIN 358 and SMC N73, possess an SED peak between 0.8 and 1.7 μm, whereas D or D' type symbiotic stars possess a peak at longer wavelengths or a flat profile respectively (Akras et al. 2019). Orbital periods for symbiotic binaries are typically between 1 and 3 years, but can be larger (Skopal 2005).

Observational data for both of these binaries were obtained from the Strasbourg astronomical Data Center (CDS) portal. Fluxes and their errors were converted from Jy to erg/cm^2/s/Å, and the frequency in GHz was converted to wavelength in angstroms. Only observations with flux errors were used. Since some filters had multiple observations, either from multiple surveys or citations, the fluxes for a given wavelength were averaged and their errors propagated.

In this section, the fitting pipeline described in 3.1, WHACCKEY PAR, will be applied to these objects to calculate the radius and mass of the giant, and the temperature and radius of the white dwarf in the binary. *The Joker* (see §3.3) will be used to find values for the period, eccentricity, velocity semi-amplitude, systemic velocity, and mass of the white dwarf in the binary.

The distance modulus for the Small Magellanic Cloud (SMC) μ and error $\delta\mu$ used was 19.01 ± 0.08 from Marconi et al. (2017). This value was chosen because it was the most recent distance modulus for the SMC found using Cepheids on the NASA/IPAC Extragalactic Database[1]. Using the equations $d = 10^{\frac{\mu}{5}+1}$ and $\delta d = 0.461 d \delta\mu$ where d is the distance in parsecs and δd is its error, the distance to the SMC used in all calculations of radius from the scaling factor is 63.4 ± 2.3 kpc.

[1] The NASA/IPAC Extragalactic Database (NED) is funded by the National Aeronautics and Space Administration and operated by the California Institute of Technology.

Table 2 contains a summary of the characteristics of the stars in LIN 358 and SMC N73. Table 3 contains a summary of the orbital parameters from *The Joker*.

4.1. *LIN 358*

There were 30 different wavelengths with flux errors for LIN 358 available on CDS. The binary LIN 358 has been a known supersoft X-ray source (SSS) for more than 10 years (Skopal 2015). According to Muerset et al. (1997), the supersoft nature of LIN 358 means it has an α-type X-ray spectrum. For α-type X-ray sources, nearly all of the X-ray flux likely comes from the WD, or hot star's, photosphere.

Akras et al. (2019) found a temperature for the giant star primary of 3768 K. Muerset et al. (1996) found a temperature of 4000 K and radius of $150R_{\odot}$, and classified the giant as a mid K spectral type star. Skopal (2015) found a best fit with a giant temperature of 4000 ± 200 and radius $178R_{\odot}$.

For the WD, Muerset et al. (1996) found a temperature of 140,000 K and a radius of $0.11R_{\odot}$. Vogel & Nussbaumer (1995) estimated the WD temperature to be within the range of 150,000-175,000 K. Kahabka & Haberl (2006) observed LIN 358 with *XMM-Newton* on 2003 November 16/17 and found a WD temperature of $227,500 \pm 30,000$ K and radius of $0.23^{+0.08}_{-0.04}R_{\odot}$. Using the same observations as Kahabka & Haberl (2006), Orio et al. (2007) found a temperature of 232,000 K and radius of $0.16R_{\odot}$. Skopal (2015), who modeled from the supersoft X-rays to the near-IR, found the best fitting WD model to be one with a temperature of 250,000 K and radius $0.09R_{\odot}$.

4.1.1. *WHACCKEY PAR Results*

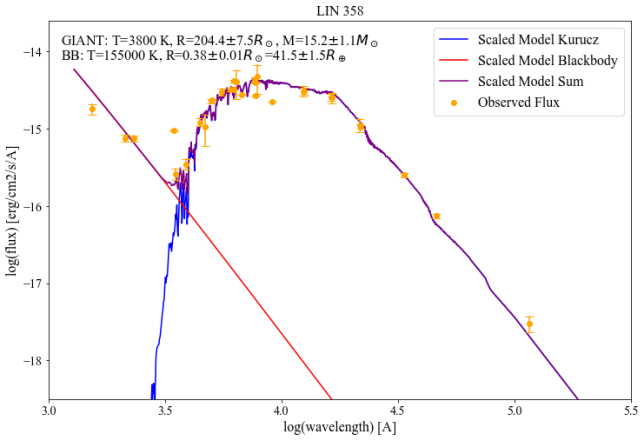

Figure 3. SED for LIN 358 with the models fitted to the observations. See 4.3 for more details.

The APOGEE values for the giant based on the 12 visits to the binary are: $T_{eff} = 3800$ K, $\log(g) = 1.0$, and metallicity [Fe/H]=0.0. The closest temperature available for the Kurucz synthetic spectra and photometry was 3750 K, so this was the model used in the χ^2 tests. The radius calculated for the giant was $204.4 \pm 7.5R_{\odot}$, and the mass was $15.2 \pm 1.1M_{\odot}$. The scaling band that produced a minimum $\chi^2 = 23.0$ is WISE $W1$.

Save for the XMM-OTT U flux, which is an outlier excluded from the blackbody fit, the Kurucz spectrum largely fits the data well within errors. The APOGEE temperature for the giant in LIN 358 is only 32 K greater than the value found by Akras et al. (2019), 3768 K. It is exactly at the lower end of error for the Skopal (2015) value, 4000 ± 200 K. The APOGEE temperature is 200 K less than the Muerset et al. (1996) value, 4000 K, but the measurement is 24 years old at the time of writing this thesis. The calculated radius is greater than both radii found by Muerset et al. (1996) and Skopal (2015). The radius from Muerset et al. (1996), $150R_{\odot}$, is over twenty years old, which means improvements in technology and subsequent increased accuracy of observations could play a role in the discrepancy. As for the radius given by WHACCKEY PAR being greater than the Skopal (2015) value, $178R_{\odot}$, their study utilized different data sets (specifically from XMM-Newton, FUSE, and HST) and also considered a nebular contribution to the total flux that was subtracted from the SED. Since WHACCKEY PAR does not consider nebular flux, this could facilitate a need for a larger star to produce the observed flux.

The temperature for the white dwarf in LIN 358 calculated by WHACCKEY PAR was 155,000 K, and the radius was $0.38 \pm 0.01R_{\odot} = 41.5 \pm 1.5R_{\oplus}$. The scaling band that produced a minimum $\chi^2 = 30.1$ was GALEX NUV. For the fit, the outlier point of flux XMM-OTT U was excluded. It is unknown why this point does not follow the general trend of the SED, but it could come from a nebular contribution to the flux.

The blackbody model fitted by WHACCKEY PAR overshoots the GALEX FUV flux and also has the largest χ^2, meaning it fits the observational data the poorest. Despite this relatively poor fit, the model temperature of 155,000 K is only 15,000 K greater than the Muerset et al. (1996) value of 140,000 and is within the range of 150,000-175,000 K estimated by Vogel & Nussbaumer (1995). The temperatures of $227,500 \pm 30,000$, 232,000 K, and 250,000 K found by Kahabka & Haberl (2006), Orio et al. (2007), and Skopal (2015) respectively were above the blackbody model temperature upper limit of 200,000 K in WHACCKEY PAR. This could explain why the radius given by WHACCKEY PAR was

about $0.1 - 0.2R_\odot$ larger than the literature values of $0.11R_\odot$ (Muerset et al. 1996), $0.23^{+0.08}_{-0.04}R_\odot$ (Kahabka & Haberl 2006), $0.16R_\odot$ (Orio et al. 2007), and $0.09R_\odot$ (Skopal 2015). A smaller radius and much hotter WD could produce the same flux as a WD with a larger radius and lower temperature.

4.1.2. *Joker Results*

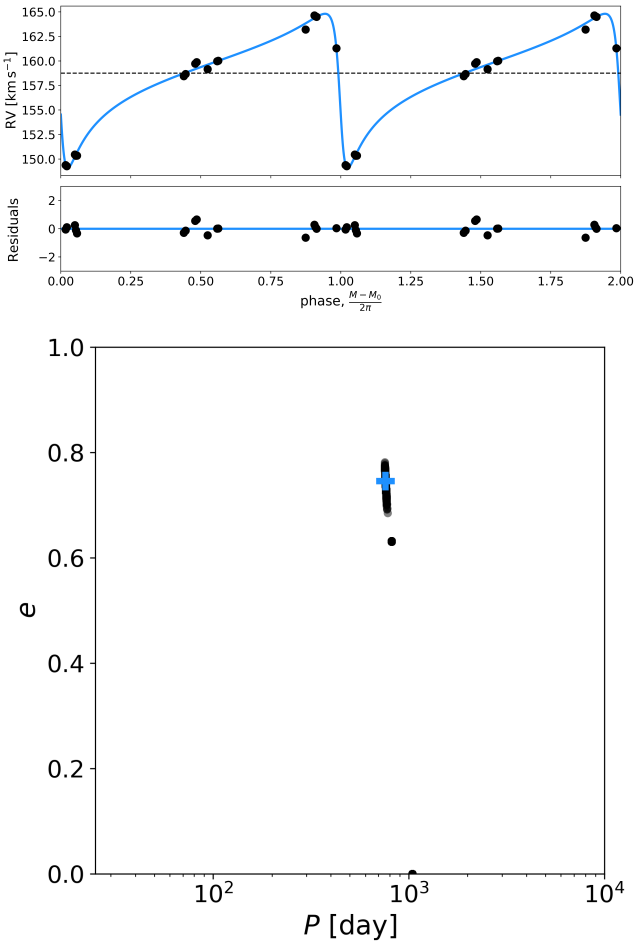

Figure 4. *Joker* results for LIN 358. See 4.3 for more details.

The Joker (see §3.3 for more details) found the most likely period is $P = 760 \pm 117$ days with a minimum allowed period of ~ 750 days and a maximum of ~ 1050 days. The eccentricity of the orbit is $e = 0.8 \pm 0.3$. The velocity semi-amplitude $K = 7.9 \pm 0.5$ km/s and the systemic velocity of LIN 358 within the SMC is $v_0 = 158.8 \pm 1.3$ km/s. The mass of the WD is $0.8 \pm 0.2M_\odot$.

The top part of Figure 4 shows that 256 posterior samples were able to be fitted to the radial velocity measurements extremely well, meaning the period is well constrained. Especially compared to Figure 6, the possible periods for LIN 358 all have nearly the same horizontal component. The most likely period, 760 days or 2.1 years, is within the typical range of 1 to 3 years given by Skopal (2005). As there is no previous literature on the period of LIN 358, this is quite exciting. The eccentricity, e, is also better constrained than the value for SMC N73. This is also visually apparent in the bottom half of Figure 4, as the values are spread out more vertically compared to the spread in period but still less so than the posterior samples of SMC N73. The most likely eccentricity, 0.8, means the orbit of LIN 358 is highly elliptical. This could cause variable X-ray emission as the white dwarf accretes at different rates based on how close the giant is to the WD in the orbit.

4.2. *SMC N73*

There exists comparatively less literature where models are fitted to the SED of SMC N73. There were only 24 different wavelengths with errors for SMC N73, and there is a noticeable gap in the SED between 2314 Å and 4445 Å where the giant and WD are both contributing to the flux.

For the giant star primary in this system, Akras et al. (2019) found an effective temperature of 3814 K, while Muerset et al. (1996) found a temperature of 3850 K and a radius of $150R_\odot$. They classified the giant as a K7 spectral type star. Muerset et al. (1996) found a white dwarf temperature of $130,000 \pm 10,000$ K and radius of $0.10R_\odot$.

4.2.1. *WHACCKEY PAR Results*

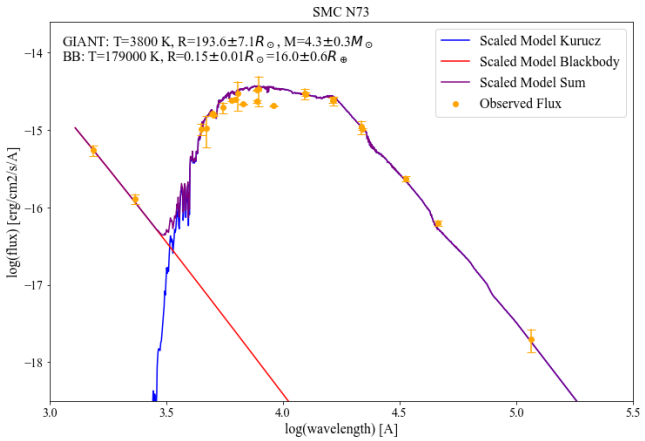

Figure 5. SED for SMC N73 with the models fitted to the observations. See 4.3 for more details.

The APOGEE values for the giant based on the 6 visits to the binary are: $T_{eff} = 3800$ K, $\log(g) = 0.5$, and [Fe/H]=-1.0. Again, since the closest temperature available for the Kurucz synthetic spectra and photometry

was 3750 K, this was the model used in the χ^2 tests. The radius calculated for the giant was $193.6 \pm 7.1 R_\odot$, and the mass was $4.3 \pm 0.3 M_\odot$. The scaling band that produced a minimum $\chi^2 = 9.4$ was 2MASS K_s.

The APOGEE temperature of 3800 K is only 14 K less than the temperature found by Akras et al. (2019), 3814 K, and 50 K less than the temperature found by Muerset et al. (1996), 3850 K. The Muerset et al. (1996) value for radius, $150 R_\odot$ is outside of the error range of the WHACCKEY PAR value $193.6 \pm 7.1 R_\odot$.

The temperature for the white dwarf in SMC N73 calculated by WHACCKEY PAR was 179,000 K, and the radius was $0.15 \pm 0.01 R_\odot = 16.0 \pm 0.6 R_\oplus$. The scaling band that produced a minimum $\chi^2 = 9.5e-7$ was GALEX NUV.

Perhaps because it is only fitting two points, the model for a 179,000 K blackbody appears to fit the UV contribution perfectly. However, this temperature is outside the error range of the Muerset et al. (1996) value of $130,000 \pm 10,000$ K. The Muerset et al. (1996) radius, $0.10 R_\odot$, is outside the error range of the WHACCKEY PAR value, $0.15 \pm 0.01 R_\odot$.

This general disagreement between the values from WHACCKEY PAR and Muerset et al. (1996) could partially be a result of updated data and improved instrumentation reducing random error and providing more accurate measurements of flux for the values used in WHACCKEY PAR. That the only easily found literature on this interesting symbiotic system is two years older than the author of this thesis emphasizes the need for future observations.

4.2.2. *Joker Results*

For SMC N73, *The Joker* found the most likely period to be $P = 777 \pm 845$ days with a minimum allowed period of ~85 days and a maximum of ~5100 days. The eccentricity of the orbit is $e = 0.0 \pm 0.2$. The velocity semi-amplitude $K = 15.7 \pm 8.9$ km/s and the systemic velocity within the SMC is $v_0 = 143.6 \pm 4.9$ km/s. The mass of the WD was simply found to be less than $1 M_\odot$.

The top half of Figure 6 shows that the 256 posterior samples were unable to fit the six epochs nearly as well as LIN 358 (top part of Fig. 4). This could be because SMC N73 has a long period so the epochs were too close together, or the period is shorter than the time between the two groups of three observations, as shown by the minimum allowed period of 85 days and maximum of 5100. The best fitting period, 777 days or 2.1 years, fits within the expected orbital period range of 1 to 3 years (Skopal 2005). The large error of 845 days is visualized in the bottom half of Figure 6, as the posterior samples are much less closely spaced on the horizontal axis than

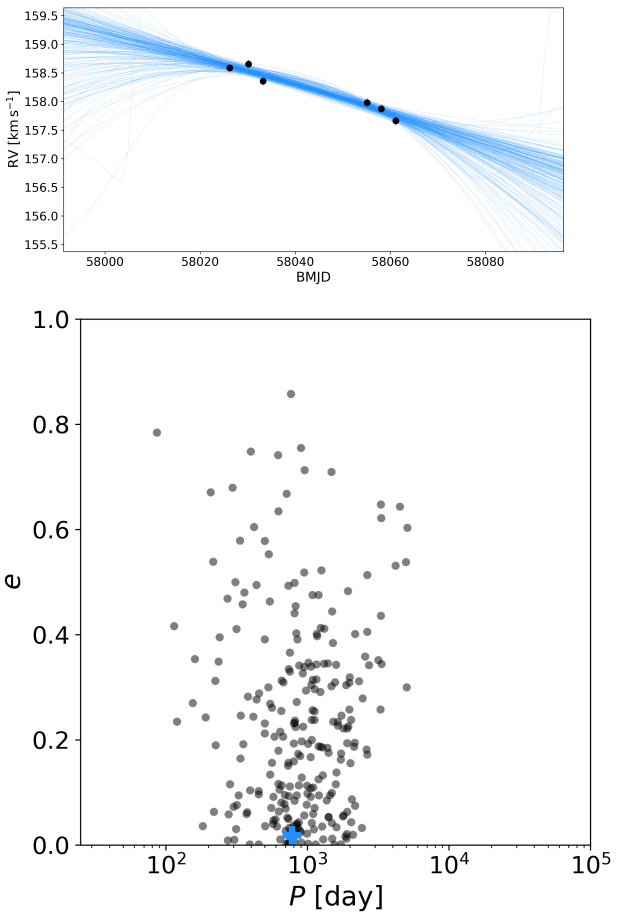

Figure 6. *Joker* results for SMC N73. See 4.3 for more details.

for LIN 358 in Figure 4. The error for e for SMC N73 is also visualized, as points are spread out on the vertical axis. Since the most likely eccentricity is 0.0, the orbit is most likely circular, unlike the highly elliptical orbit of LIN 358. Because v_0, 143.6 ± 4.8 km/s, is smaller than the systemic velocity of LIN 358, 158.8 ± 1.3 km/s, SMC N73 is located further from the center of the SMC.

4.3. *Explanation of Figures*

Figures 3 and 5 show the SED for each binary with the models fitted to the observations (orange). The red line is the blackbody/WD model, blue represents the Kurucz synthetic spectrum for the giant, and the purple curve is their sum.

Figures 4 and 6 show graphs created by *The Joker*. The top graph shows the APOGEE visit velocity data (black markers; error bars are shown, but are typically smaller than the marker) and the radial velocity orbits computed from the posterior samples (blue lines). The bottom graph shows the 256 posterior samples in period

P and eccentricity e. The blue cross-hairs indicate the maximum a posterior (or MAP) sample, which is the most likely orbit.

5. CONCLUSIONS

We find that the methodology used to create the APOGEE-GALEX-*Gaia* SN Ia Progenitor catalog is effective for finding promising WD-MS candidates that could be Cataclysmic Variable systems. Further investigation of the sources with Type 1 and Variable 1 SEDs already led to the confirmation of LIN 358 and SMC N73 as systems with extremely hot stellar components. This classification will also improve efficiency of any follow-up efforts with these sources. However, because the observed UV flux was not removed from the points considered in the Virtual Observatory fitting of the BT-Settl-CIFIST main sequence star models to the SEDs, visual classification of the 1470 candidates should be redone with FUV and NUV excluded. This may result in the reclassification of some Type 2 and Variable 2 SEDs to Type 1 and Variable 1 SEDs, increasing the number of potential CVs.

It was also found that the Python SED fitting pipeline WHACCKEY PAR was able to reasonably characterize the giant and WD within LIN 358 and SMC N73. According to WHACCKEY PAR, LIN 358 is composed of a 3800 K giant with radius $204.4 \pm 7.5 R_{\odot}$ and mass $15.2 \pm 1.1 M_{\odot}$ and a 155,000 K WD with radius $0.38 \pm 0.01 R_{\odot} = 41.5 \pm 1.5 R_{\oplus}$. *The Joker* gives a WD mass of $0.8 \pm 0.2 M_{\odot}$ for this system. SMC N73 is composed of a 3800 K giant with radius $193.6 \pm 7.1 R_{\odot}$ and mass $4.3 \pm 0.3 M_{\odot}$ and a 179,000 K WD with radius $0.15 \pm 0.01 R_{\odot} = 16.0 \pm 0.6 R_{\oplus}$. *The Joker* gives a WD mass of less than $1 M_{\odot}$ for this system.

The final χ^2 values for the SED model fitting performed by WHACCKEY PAR ranged from $9.5e-7$ to 30.1, and were affected by factors such as number of points fitted (the smallest χ^2 only summed two points) and outlier points causing large differences despite the model generally fitting the data well. Comparisons of WHACCKEY PAR values with those of previous literature varied in levels of agreement. We found the APOGEE temperatures of both giants were comparable to previous literature values, but all radii given by WHACCKEY PAR were greater than values in literature. Potential causes for this include age of the data in Muerset et al. (1996) and the differing method for finding giant star parameters in Skopal (2015). The two smallest χ^2 values were for the giant and WD in SMC N73, showing that WHACCKEY PAR was better able to characterize this binary than LIN 358.

There is plenty of future work that can be done to improve WHACCKEY PAR. A version that fits a sum of the two models instead of individually fitting the two objects could provide better results, as all observations are used in the χ^2 instead of a small range. Alternatively, the flux for the giant could be subtracted from the SED for the system and the blackbody fitted to the remaining flux. Also, for LIN 358 Skopal (2015) considers a nebular flux along with the contributions of the WD and giant to the SED. Future versions of WHACCKEY PAR could add nebular models to account for this potential contribution in symbiotic stars, and may produce a better fit for the blackbody/WD. The blackbody models in Skopal (2015) also go above 200,000 K whereas the Virtual Observatory blackbody synthetic photometry used by WHACCKEY PAR does not, so an increased temperature range could be valuable. The temperature of the best fitting model did not have an error attached due to time constraints, but would be another useful and important future addition to the pipeline.

Using *The Joker*, we found a well constrained period for LIN 358. There is no previous literature on the period of this system, so this is a significant discovery. SMC N73 orbital parameters had much larger standard deviations in the 256 posterior samples, meaning it was not able to be well constrained using *The Joker*. LIN 358 has a most likely eccentricity of 0.8, meaning the orbit is highly elliptical and may contribute to variable X-ray emission. The smaller systemic velocity v_0 of SMC N73 compared to LIN 358 shows that SMC N73 is further from the center of the SMC.

Further observation of N73 would be beneficial for better characterizing the system, as there is a gap in the flux data between 2314 and 4445 Å where both stars are significantly contributing to the observed flux in the SED. Observations at wavelengths within this gap would provide more data for the blackbody model fit so that the χ^2 would sum over more than two data points. More radial velocity measurements of the system would help with characterization of the system with *The Joker*, specifically finding better estimates for the orbital parameters. Further observations could potentially reveal that SMC N73 is an X-ray source like LIN 358 and Draco C-1. While not as immediately attractive as the known X-ray source LIN 358, SMC N73 is still a fascinating symbiotic star system with a very hot WD that could provide insight into Cataclysmic Variable systems and in turn Type Ia supernova progenitors.

BINARY		T_{eff}	R [$R_\odot$]	error	M [$M_\odot$]	error
LIN 358	GIANT	3800	204.4	7.5	15.2	1.1
	WD	155000	0.38	0.01	0.8^a	0.2^a
SMC N73	GIANT	3800	193.6	7.1	4.3	0.3
	WD	179000	0.15	0.01	$< 1.0^a$	N/A

Table 2. Temperature, radii, and masses of stars in LIN 358 and SMC N73. Unless otherwise stated, values are from the Python model fitting pipeline WHACCKEY PAR.

[a]Found using *The Joker* (Price-Whelan et al. 2017).

BINARY	P (days)	error	e	error	K [km/s]	error	v_0 [km/s]	error
LIN 358	760	117	0.8	0.3	7.9	0.5	158.8	1.3
SMC N73	777	845	0.0	0.2	15.7	8.9	143.6	4.9

Table 3. Period, eccentricity, velocity semi-amplitude, and systemic velocity of the binary from The Joker (Price-Whelan et al. 2017).

ACKNOWLEDGMENTS

I would like to thank my advisor Professor Majewski for all of the feedback on this thesis, and also for putting up with all my joke titles. I would like to thank my other advisor, Dr. Borja Anguiano, for always maintaining morale and also liking all of my joke titles, and Hannah Lewis for all her help with *The Joker*. I would also like to thank my family for their support in my pursuit of astronomy long before I was a UVA undergraduate student.

This research has made use of the New Online Database of Symbiotic Variables.

This publication makes use of VOSA, developed under the Spanish Virtual Observatory project supported by the Spanish MINECO through grant AyA2017-84089. VOSA has been partially updated by using funding from the European Union's Horizon 2020 Research and Innovation Programme, under Grant Agreement nº 776403 (EXOPLANETS-A).

This research has made use of the NASA/IPAC Extragalactic Database (NED), which is funded by the National Aeronautics and Space Administration and operated by the California Institute of Technology.

This research is based on observations made with the Galex Evolution Explorer, obtained from the MAST data archive at the Space Telescope Science Institute, which is operated by the Association of Universities for Research in Astronomy, Inc., under NASA contract NAS 5–26555.

Funding for the Sloan Digital Sky Survey IV has been provided by the Alfred P. Sloan Foundation, the U.S. Department of Energy Office of Science, and the Participating Institutions. SDSS-IV acknowledges support and resources from the Center for High-Performance Computing at the University of Utah. The SDSS web site is www.sdss.org.

SDSS-IV is managed by the Astrophysical Research Consortium for the Participating Institutions of the SDSS Collaboration including the Brazilian Participation Group, the Carnegie Institution for Science, Carnegie Mellon University, the Chilean Participation Group, the French Participation Group, Harvard-Smithsonian Center for Astrophysics, Instituto de Astrofísica de Canarias, The Johns Hopkins University, Kavli Institute for the Physics and Mathematics of the Universe (IPMU) / University of Tokyo, the Korean Participation Group, Lawrence Berkeley National Laboratory, Leibniz Institut für Astrophysik Potsdam (AIP), Max-Planck-Institut für Astronomie (MPIA Heidelberg), Max-Planck-Institut für Astrophysik (MPA Garching), Max-Planck-Institut für Extraterrestrische Physik (MPE), National Astronomical Observatories of China, New Mexico State University, New York University, University of Notre Dame, Observatário Nacional / MCTI, The Ohio State University, Pennsylvania State University, Shanghai Astronomical Observatory, United Kingdom Participation Group, Universidad Nacional Autónoma de México, University of Arizona, University of Colorado Boulder, University of Oxford, University of Portsmouth, University of Utah, University of Virginia, University of Washington, University of Wisconsin, Vanderbilt University, and Yale University.

This work has made use of data from the European Space Agency (ESA) mission *Gaia* (https://www.cosmos.esa.int/gaia), processed by the *Gaia* Data Processing and Analysis Consortium (DPAC, https://www.cosmos.esa.int/web/gaia/dpac/consortium). Funding for the DPAC has been provided by national institu-

tions, in particular the institutions participating in the *Gaia* Multilateral Agreement.

This research has made use of the SIMBAD database, operated at CDS, Strasbourg, France

REFERENCES

Akras, S., Guzman-Ramirez, L., Leal-Ferreira, M. L., & Ramos-Larios, G. 2019, ApJS, 240, 21, doi: 10.3847/1538-4365/aaf88c

Astropy Collaboration, Robitaille, T. P., Tollerud, E. J., et al. 2013, A&A, 558, A33, doi: 10.1051/0004-6361/201322068

Baraffe, I., Homeier, D., Allard, F., & Chabrier, G. 2015, A&A, 577, A42, doi: 10.1051/0004-6361/201425481

Bayo, A., Rodrigo, C., Barrado Y Navascués, D., et al. 2008, A&A, 492, 277, doi: 10.1051/0004-6361:200810395

Bianchi, L., Shiao, B., & Thilker, D. 2017, ApJS, 230, 24, doi: 10.3847/1538-4365/aa7053

Castelli, F., Gratton, R. G., & Kurucz, R. L. 1997, A&A, 318, 841

Gaia Collaboration, Brown, A. G. A., Vallenari, A., et al. 2018, A&A, 616, A1, doi: 10.1051/0004-6361/201833051

Kahabka, P., & Haberl, F. 2006, A&A, 452, 431, doi: 10.1051/0004-6361:20054207

Kinman, T. D., & Brown, W. R. 2014, AJ, 148, 121, doi: 10.1088/0004-6256/148/6/121

Kolenberg, K., Fossati, L., Shulyak, D., et al. 2010, A&A, 519, A64, doi: 10.1051/0004-6361/201014471

Kurucz, R. 1993, ATLAS9 Stellar Atmosphere Programs and 2 km/s grid. Kurucz CD-ROM No. 13. Cambridge, 13

Majewski, S. R., Schiavon, R. P., Frinchaboy, P. M., et al. 2017, AJ, 154, 94, doi: 10.3847/1538-3881/aa784d

Marconi, M., Molinaro, R., Ripepi, V., et al. 2017, MNRAS, 466, 3206, doi: 10.1093/mnras/stw3289

Merc, J., Gális, R., & Wolf, M. 2019, Research Notes of the American Astronomical Society, 3, 28, doi: 10.3847/2515-5172/ab0429

Morrissey, P., Conrow, T., Barlow, T. A., et al. 2007, ApJS, 173, 682, doi: 10.1086/520512

Muerset, U., Schild, H., & Vogel, M. 1996, A&A, 307, 516

Muerset, U., Wolff, B., & Jordan, S. 1997, A&A, 319, 201

Orio, M., Zezas, A., Munari, U., Siviero, A., & Tepedelenlioglu, E. 2007, ApJ, 661, 1105, doi: 10.1086/514806

Price-Whelan, A. M., Hogg, D. W., Foreman-Mackey, D., & Rix, H.-W. 2017, ApJ, 837, 20, doi: 10.3847/1538-4357/aa5e50

Price-Whelan, A. M., Hogg, D. W., Rix, H.-W., et al. 2020, arXiv e-prints, arXiv:2002.00014. https://arxiv.org/abs/2002.00014

Rodríguez-Merino, L. H., Chavez, M., Bertone, E., & Buzzoni, A. 2005, ApJ, 626, 411, doi: 10.1086/429858

Skopal, A. 2005, A&A, 440, 995, doi: 10.1051/0004-6361:20034262

—. 2015, NewA, 36, 116, doi: 10.1016/j.newast.2013.10.009

Vogel, M., & Nussbaumer, H. 1995, A&A, 301, 170

Wall, R. E., Kilic, M., Bergeron, P., et al. 2019, MNRAS, 489, 5046, doi: 10.1093/mnras/stz2506